

XY Spin Fluid in an External Magnetic Field

I. P. Omelyan,^{1,2} W. Fenz,² I. M. Mryglod,^{1,2} and R. Folk,²

¹*Institute for Condensed Matter Physics, 1 Svientsitskii Street, UA-79011 Lviv, Ukraine*

²*Institute for Theoretical Physics, Linz University, A-4040 Linz, Austria*

(June 19, 2018)

A method of integral equations is developed to study inhomogeneous fluids with planar spins in an external field. As a result, the calculations for these systems appear to be no more difficult than those for ordinary homogeneous liquids. The approach proposed is applied to the ferromagnetic XY spin fluid in a magnetic field using a soft mean spherical closure and the Born-Green-Yvon equation. This provides an accurate reproduction of the complicated phase diagram behavior obtained by cumbersome Gibbs ensemble simulation and multiple histogram reweighting techniques.

PACS number(s): 05.70.Fh, 64.60.-i, 64.70.Fx, 75.50.Mm

Spin fluids are examples of many body systems showing a *rich* variety of phases in the global phase diagram [1–4]. Besides gas-liquid (G-L) and para-ferro-magnetic (P-F) phase transitions, tricritical, critical end and triple point behavior is observed. Under special conditions, an unsymmetrical tricritical van Laar point exists additionally [5]. This complexity arises due to a *coupling* between spin and spatial interactions. Similar phase diagrams are found in symmetric binary mixtures [6–10] with their demixing and G-L transitions, spin lattice gas models [11,12], mixtures of ³He-⁴He with the superfluid and demixing states [13–15], and other systems.

The properties of spin fluids were studied using mean field (MF) theories [1–4], more accurate integral equation (IE) approaches [5,16–20], and Monte Carlo (MC) simulation techniques [4,16,19,21–24]. Different types of models, such as the well-recognized discrete 1D spin Ising, or continuous 2D spin XY and 3D Heisenberg fluids, have been considered. Despite this, the question concerning the global phase diagram topology of the XY spin fluid including the influence of an external magnetic field has *never* been addressed. Moreover, the IE approach has been restricted either to simplified ideal Heisenberg fluids [16–20], where nonmagnetic attractive interactions are absent, or to ideal and nonideal Ising models [5].

Surprisingly, up to now there were *no* attempts on developing the IE approach for the XY spin fluid model. This model may play a crucial role in the description of superfluid transitions in pure ⁴He and its mixtures in bulk or in media such as porous gold [15] or silica aerogel [25]. It is generally believed [25] that the superfluid transition in ⁴He belongs to the classical 3D XY model universality class (here 3D relates to the dimensionality of spatial coordinates). On the other hand, the fluid of particles with embedded XY spins described by classical statistical mechanics can be treated as one of the simplest model of disordered continuum systems exhibiting ferromagnetic behavior.

The presence of spin interactions and external fields destroys the homogeneity of the fluid, producing nonuniformity or *anisotropy* in the one-body density. Within the standard IE approach this leads to the necessity of

performing very complicated joint calculations for one- and two-body distribution functions on the basis of the coupled set of the *inhomogeneous* Ornstein-Zernike (IOZ) equation, a closure relation, and the first equation of the Born-Green-Yvon (BGY) hierarchy [26]. Such calculations result in *unresolvable* numerical difficulties because of the restricted capabilities of modern supercomputers. It is worth emphasizing also that existing IE developments for Ising [5] and Heisenberg [16–20] systems are not applicable to the XY fluid. The reason is that neither it can be mapped onto a binary homogeneous mixture (as for Ising) nor its anisotropic correlations be expanded in spherical harmonics (as for Heisenberg). The specific XY spin interactions require a separate IE consideration.

In this Letter we present a method allowing to overcome the difficulties of the IOZ approach in the case of XY fluids. Comparison of the obtained IE solutions with our simulation results has shown a quantitative reproduction of the phase diagrams in a wide region of temperature, density, external field and interaction parameters.

Consider an XY spin fluid model with the Hamiltonian

$$U = \sum_{i < j}^N \left[\phi(r_{ij}) - I(r_{ij}) - J(r_{ij}) \mathbf{s}_i \cdot \mathbf{s}_j \right] - \mathbf{H} \cdot \sum_{i=1}^N \mathbf{s}_i, \quad (1)$$

where N is the total number of particles, \mathbf{r}_i is the 3D spatial coordinate of the i -th body carrying 2D spin \mathbf{s}_i of unit length, $r_{ij} = |\mathbf{r}_i - \mathbf{r}_j|$ denotes the interparticle separation, and \mathbf{H} is the external magnetic field vector lying like \mathbf{s}_i in the XY-plane. The exchange integral J of ferromagnetic interactions and the nonmagnetic attraction potential I can be chosen in the form of Yukawa functions,

$$J(r) = \frac{\epsilon\sigma}{r} \exp\left(-\frac{r-\sigma}{\sigma}\right), \quad I(r) = J(r)/R, \quad (2)$$

where ϵ and σ denote the interaction intensity and the size of the particles, respectively, with R being the ratio defining the relative strength of J to I . The repulsion ϕ between particles can be modeled by a more realistic soft-core (shifted Lennard-Jones) potential [4,5],

$$\phi(r) = \begin{cases} 4\epsilon \left[\left(\frac{\sigma}{r} \right)^{12} - \left(\frac{\sigma}{r} \right)^6 \right] + \epsilon, & r < \sqrt[6]{2}\sigma, \\ 0, & r \geq \sqrt[6]{2}\sigma, \end{cases} \quad (3)$$

rather than by the hard sphere one.

A complete thermodynamic and magnetic description of system (1) can be performed in terms of orientationally dependent one-body $\xi(\varphi)$ and two-body $g(r, \varphi_1, \varphi_2) = h(r, \varphi_1, \varphi_2) + 1$ distribution functions. The angles φ are referred to the external field, so that $\mathbf{H} \cdot \mathbf{s} = H \cos \varphi$ and $\mathbf{s}_1 \cdot \mathbf{s}_2 = \cos(\varphi_1 - \varphi_2)$. According to the liquid state theory [26], the total correlation function h satisfies the IOZ equation which in our case reads

$$h(r, \varphi_1, \varphi_2) = c(r, \varphi_1, \varphi_2) + \frac{\rho}{2\pi} \int_V \mathbf{dr}' \int_0^{2\pi} d\varphi \times \xi(\varphi) c(|\mathbf{r} - \mathbf{r}'|, \varphi_1, \varphi) h(r', \varphi, \varphi_2), \quad (4)$$

where $\rho = N/V$ is the particle number density, V the volume and $c(r, \varphi_1, \varphi_2)$ the direct correlation function.

The IOZ equation (4) must be complemented by a closure relation. The most general form of it is

$$g = \exp(-\beta u + h - c + B), \quad (5)$$

where $u(r, \varphi_1, \varphi_2) = \phi(r) - I(r) - J(r) \cos(\varphi_1 - \varphi_2)$ with $\beta^{-1} = k_B T$ being the temperature, and B is the bridge function. This function cannot be determined exactly for *any* system of interacting particles, but a lot of approaches exist allowing to present it approximately [26]. One way is to use the soft mean spherical approximation (SMSA) [5,27]

$$B(r, \varphi_1, \varphi_2) = \ln[1 + \tau(r, \varphi_1, \varphi_2)] - \tau(r, \varphi_1, \varphi_2), \quad (6)$$

where $\tau = h - c - \beta u_1$. The long-ranged part u_1 can be extracted [5] from the total potential u as $u_1(r, \varphi_1, \varphi_2) = -[I(r) + J(r) \cos(\varphi_1 - \varphi_2)] \exp[-\beta \phi(r)]$.

Evaluation of pair correlations from IOZ equation (4) requires the knowledge of $\xi(\varphi)$. The latter is obtained from the first member of the BGY hierarchy [26],

$$\frac{d}{d\varphi} \ln \xi(\varphi) = \frac{d}{d\varphi} \beta H \cos \varphi - \beta \frac{\rho}{2\pi} \int_V \mathbf{dr} \int_0^{2\pi} d\varphi' \times \xi(\varphi') g(r, \varphi, \varphi') \frac{du(r, \varphi, \varphi')}{d\varphi'}. \quad (7)$$

Eqs. (4), (5), and (7) constitute a very complicated set of coupled IOZ/SMSA/BGY nonlinear integro-differential equations with respect to h (or g), c , and ξ . The main problem in solving it is that the unknowns h and c depend on up to three variables. This leads to unresolvable numerical difficulties, and thus a method is needed to remedy such a situation.

Any periodic function of two angle variables can be expanded in sine and cosine harmonics as

$$f(r, \varphi_1, \varphi_2) = \sum_{n,m=0}^{\infty} \sum_{l,l'=0,1} f_{nml'l'}(r) T_{nl}(\varphi_1) T_{ml'}(\varphi_2) \quad (8)$$

using the orthogonal Chebyshev polynomials $T_{n0}(\varphi) = \cos(n\varphi)$ and $T_{n1}(\varphi) = -\frac{1}{n} dT_{n0}(\varphi)/d\varphi = \sin(n\varphi)$. Expansion (8) can readily be applied to our two-body functions $\{h, g, c\} \equiv f$ with the simplification $f_{nml'l'} = f_{nml} \delta_{ll'}$ because they are invariant with respect to the transformation $(\varphi_1, \varphi_2) \leftrightarrow (-\varphi_1, -\varphi_2)$ in view of the symmetry of Hamiltonian (1). Then exploiting the orthonormality condition $\int_0^{2\pi} T_{nl}(\varphi) T_{ml'}(\varphi) d\varphi = t_n \delta_{nm} \delta_{ll'}$, where $t_n = \pi(1 - \delta_{n0}) + 2\pi \delta_{n0}$, yields the expansion coefficients

$$f_{nml}(r) = \frac{1}{t_n t_m} \iint f(r, \varphi_1, \varphi_2) T_{nl}(\varphi_1) T_{ml}(\varphi_2) d\varphi_1 d\varphi_2. \quad (9)$$

In terms of these coefficients the IOZ equation (4) reduces to

$$h_{nml}(k) = c_{nml}(k) + \rho \sum_{n',m'} c_{nm'l'}(k) \xi_{n'm'l} h_{n'm'l}(k), \quad (10)$$

where $\xi_{nml} = \frac{1}{2\pi} \int_0^{2\pi} \xi(\varphi) T_{nl}(\varphi) T_{ml}(\varphi) d\varphi$ are the moments of $\xi(\varphi)$, and the 3D Fourier transform $f(k) = \int_V f(r) \exp(i\mathbf{k} \cdot \mathbf{r}) d\mathbf{r}$ has been used. The algebraic representation (10) looks like the OZ equation corresponding to a mixture of ordinary *homogeneous* fluids. This is a very important feature because the problem can now be solved by adapting algorithms already *known* for homogeneous systems.

Furthermore, we perform the one-body polynomial expansion

$$\ln \xi(\varphi) = \beta H \cos \varphi + \sum_{n=0}^{\infty} a_n T_{n0}(\varphi), \quad (11)$$

where only cosine harmonics appear due to the property $\xi(-\varphi) = \xi(\varphi)$. Then the cumbersome integro-differential equation (7) allows to be solved analytically,

$$a_n = \frac{\beta \rho}{2n} \int_V \mathbf{dr} \sum_{m=0}^{\infty} \sum_{l,l'=0,1} (-1)^{l+l'} \xi_{m1l} g_{n-1+2l'ml}(r) J(r) \quad (12)$$

for $n \geq 1$, while the coefficient a_0 is determined from the normalization $\frac{1}{2\pi} \int_0^{2\pi} \xi(\varphi) d\varphi = 1$.

Handling the SMSA closure (5) also presents no difficulties, because for distances $r \geq 2^{1/6}\sigma$ (where $\phi(r) = 0$) we obtain from Eqs. (5) and (6) that $c(r, \varphi_1, \varphi_2) = \beta[I(r) + J(r) \cos(\varphi_1 - \varphi_2)]$. Taking into account the equality $\cos(\varphi_1 - \varphi_2) = T_{10}(\varphi_1) T_{10}(\varphi_2) + T_{11}(\varphi_1) T_{11}(\varphi_2)$, one finds $c_{000}(r) = \beta I(r)$ and $c_{110}(r) = c_{111}(r) = \beta J(r)$, while all other c -coefficients will be equal to zero at $r \geq 2^{1/6}\sigma$. For $r < 2^{1/6}\sigma$, we should perform numerical integration (see Eq. (9)) of the right-hand side of Eq. (5) in order to obtain the expansion coefficients $g_{nml}(r)$.

Another important feature is that only a *small* number \mathcal{N} of harmonics should be, in fact, involved because the expansion coefficients rapidly tend to zero with increasing \mathcal{N} . Then the sums $\sum_{n,m}^{\infty}$ can be replaced without loss

of precision by finite ones with $n, m \leq \mathcal{N}$. In our case the anisotropic potential is presented by zeroth and first harmonics (see above the expansion for $\cos(\varphi_1 - \varphi_2)$), while a slight anharmonicity ($\mathcal{N} > 1$) in the correlation functions appears due to the nonlinearity of the closure.

Once the expansion coefficients are found, *all* the magnetic and thermodynamic properties of the system are obtained in a straightforward way. In particular, the pressure P can be calculated from the virial equation

$$\begin{aligned} \frac{\beta P}{\rho} &= 1 - \frac{1}{6} \frac{\beta \rho}{(2\pi)^2} \int d\mathbf{r} d\varphi_1 d\varphi_2 \xi(\varphi_1) \xi(\varphi_2) g(r, \varphi_1, \varphi_2) \\ \times r \frac{du(r, \varphi_1, \varphi_2)}{dr} &= 1 - \frac{\beta \rho}{6} \sum_{n,m} \int r d\mathbf{r} \left(\frac{d[\phi(r) - I(r)]}{dr} \right. \\ &\quad \left. \times \xi_{n00} \xi_{m00} g_{nm0}(r) - \frac{dJ(r)}{dr} \sum_{l=0,1} \xi_{n1l} \xi_{m1l} g_{nml}(r) \right), \end{aligned} \quad (13)$$

whereas the magnetization $M = \frac{1}{2\pi} \int_0^{2\pi} \cos(\varphi) \xi(\varphi) d\varphi = \xi_{100}$. Then the phase coexistence densities between gas and liquid states can be evaluated by applying the well-known Maxwell construction to Eq. (13), while the P-F transition will correspond to a boundary Curie curve in the temperature-density plane where nonzero (spontaneous) magnetization $M \neq 0$ becomes possible at $H = 0$.

The coupled set of homogeneous OZ/SMSA/BGY equations (5), (10), and (12) was solved by adapting the algorithm used in Ref. [5]. The integration with respect to angle variables has been performed by Gauss-Chebyshev quadratures. The number of harmonics involved was $\mathcal{N} = 3$. Further increase of \mathcal{N} does not affect the solutions. Other computational details are similar to those of Ref. [5] when solving the Ising IE equations. The dimensionless quantities $\rho^* = \rho\sigma^3$, $T^* = k_B T/\epsilon$, and $H^* = H/\epsilon$ were chosen in the presentation of the results.

The simulations were carried out using the Gibbs ensemble MC (GEMC) [28] and multiple histogram reweighting (MHR) [29] techniques for evaluating the G-L and liquid-liquid (L-L) coexistences, while the Binder crossing scheme [24,30] was utilized to determine the P-F magnetic transition (at $H = 0$). Other simulation details are similar to those reported in Refs. [4,5,24].

In Fig. 1 we compare the OZ/SMSA/BGY results for the *ideal* ($R = \infty$) XY fluid at different external fields H with the GEMC and MHR simulation data. At $H = 0$, a tricritical (TC) point separates the second order P-F magnetic phase transition line from the first order transition between a P-gas and an F-liquid. The H -dependence of the G-L critical temperature and density is *nonmonotonic*. Samples of the MF binodals are included in Fig. 1 as well to demonstrate the obvious advantage of the IE theory over the MF approach. Note that contrary to the theoretical binodals, the GEMC and MHR coexistence curves terminate when approaching the critical regions. This is because of the appearance of huge density fluctuations which cannot be properly handled within finite simulation boxes. The MHR technique allows to approach

to critical points more closely (see Fig. 1) and should be considered as more preferable than the GEMC method.

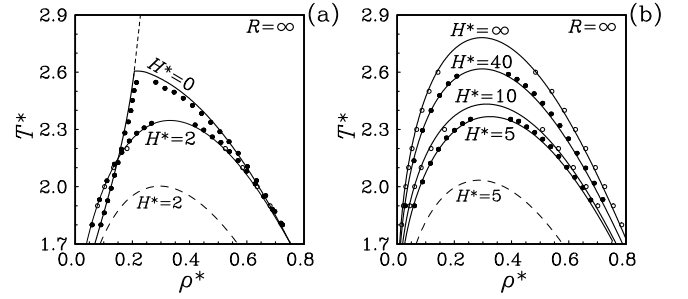


FIG. 1. The G-L binodals obtained for the ideal XY fluid within the OZ/SMSA/BGY approach (full curves) versus the GEMC (open circles) and MHR (full circles) simulation data. The P-F transition is plotted by the short-dashed line. The MF samples are shown by low lying long-dashed curves.

The OZ/SMSA/BGY and MHR phase diagrams of the *nonideal* XY-fluid are shown in Figs. 2 and 3 for different ratios R and magnetic fields H . *Four* types of phase diagram topology can be identified overall. For large $R \geq 0.415$ (type I), the system exhibits an *ideal-like* behavior with the existence of a TC point at $H = 0$ and G-L transitions at $H \neq 0$ for each R (Fig. 2(a)). At moderate values $0.26 < R < 0.415$ (type II), the transition between a P-liquid and an F-liquid arises at $H = 0$ *additionally* to the transition between a P-gas and a P-liquid. Here a triple point (TP) *occurs* too, where a rare P-gas, a moderately dense P-liquid, and a highly dense F-liquid all coexist at the same T and P (see Figs. 2(b) and 3(a)). The TPs can *exist* at $H \neq 0$ as well and describe then the phase coexistence between a weakly magnetized gas, a moderate magnetized liquid and a strongly magnetized liquid (Fig. 3(b)). With increasing H , either the G-L ($0.376 < R < 0.415$, type IIa) or L-L ($0.26 < R < 0.376$, type IIb) transition *disappears* in a critical end (CE) point at some finite H . For instance, even if R is slightly smaller than the boundary value $R_{VL} = 0.376$, namely $R = 0.37$, the L-L critical point ends at some $H^* \sim 1$, while the G-L critical point extends to infinite field (Fig. 3(a)). In the special case $R = R_{VL}$, the G-L and L-L transition lines *merge* into the TC van Laar point at $H^* = 1.9$ (Fig. 3(b)). For small $R \leq 0.26$ (type III), the translational interaction dominates over the spin one, remaining the G-L transition, whereas the TC point at $H = 0$ *transforms* into a CE point (Fig. 2(b)). For $H \rightarrow \infty$, the system at any R behaves like a *simple* fluid with $u(r) = \phi(r) - I(r) - J(r)$ (then all spins align along \mathbf{H}).

As can be seen, the agreement between the theory proposed and the simulations is *quite* satisfactory. Slight deviations appear only in the vicinity of critical points. This is explained by finite size effects in the simulations and an approximate character of the SMSA closure used in the theory. For the latter reason, the classical value $\beta = 1/2$ of the critical exponent describing the G-L bin-

odal behavior $|\rho - \rho_c| \sim |T - T_c|^\beta$ near the critical point (ρ_c, T_c) is recovered (in particular, at $R = \infty$ and $H \neq 0$), instead of the value $\beta \approx 1/3$ known from the renormalization group analysis [31]. On the other hand, the crossover to the TC value $\beta = 1/4$ can be observed near the van Laar point at $R = 0.376$ and $H^* = 1.9$ (Fig. 3(b)).

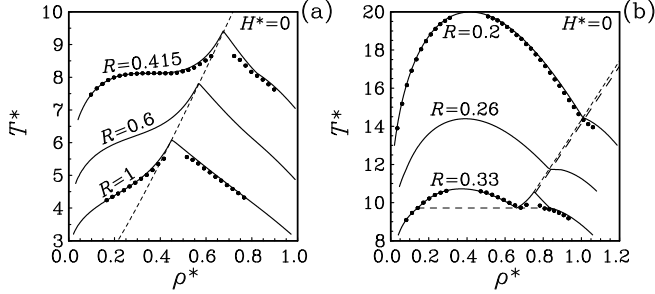


FIG. 2. The G-L and L-L binodals of the nonideal XY fluid within the OZ/SMSA/BGY approach (full curves) versus the MHR data (circles). The P-F transition is plotted by the short- (theory) and long- (simulation) dashed curves. The triple point is represented by the horizontal dashed line.

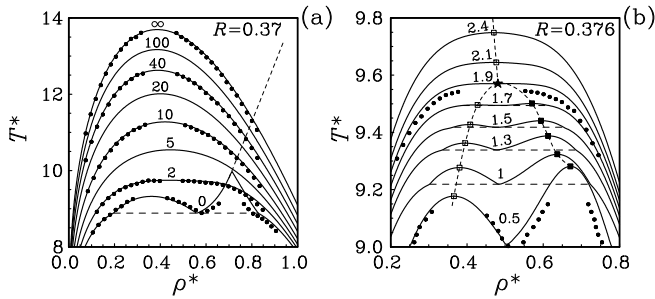


FIG. 3. The binodals near (a) and at (b) the boundary value $R = R_{vL}$. The G-L and L-L critical points are shown in subset (b) for different H^* as open and full squares, respectively, connected by dashed curves. The curves meet in the TC point (star). Other notations are the same as for Fig. 2.

More precise IE calculations near critical points are *possible* provided a more accurate closure is used. For instance, the self-consistent OZ ansatz (SCOZA) [7–9] (which in its present formulation was implemented only for simple homogeneous hard-sphere Yukawa systems) can be *extended* to our inhomogeneous soft-core XY fluid by introducing a state dependent function $K(\rho, T, H)$ into the SMSA closure. Then K is determined by the requirement of thermodynamic *consistency* between the energy and compressibility routes. In view of the inhomogeneity and softness, this leads to a significant sophistication of the calculations. They go beyond the scope of the present Letter and will be considered elsewhere.

In conclusion, we point out that a *novel* technique to study orientationally ordered fluids with planar spins has been proposed. It combines the standard IE method with appropriate expansions of the inhomogeneous correlation functions in terms of orthogonal polynomials. This reduces the calculations to those inherent in a mixture of ordinary homogeneous fluids and thus presents now *no*

numerical difficulties. Detailed comparisons with simulations have shown that the proposed approach is powerful enough to give a *quantitative* description of phase transitions in the XY spin fluid systems.

This work was supported in part by the Fonds zur Förderung der wissenschaftlichen Forschung under Project No. P15247.

- [1] P. C. Hemmer and D. Imbro, Phys. Rev. A **16**, 380 (1977).
- [2] J. M. Tavares *et al.*, Phys. Rev. E **52**, 1915 (1995).
- [3] F. Schinagl, H. Iro, and R. Folk, Eur. Phys. J. B **8**, 113 (1999).
- [4] W. Fenz *et al.*, Phys. Rev. E **68**, 061510 (2003).
- [5] I. P. Omelyan *et al.*, Phys. Rev. E **69**, 061506 (2004).
- [6] N. B. Wilding, F. Schmid, and P. Nielaba, Phys. Rev. E **58**, 2201 (1998).
- [7] G. Kahl, E. Schöll-Paschinger, and A. Lang, Monatshefte für Chemie **132**, 1413 (2001).
- [8] G. Kahl, E. Schöll-Paschinger, and G. Stell, J. Phys.: Condens. Matter **14**, 9153 (2002).
- [9] E. Schöll-Paschinger and G. Kahl, J. Chem. Phys. **118**, 7414 (2003).
- [10] D. Pini *et al.*, Phys. Rev. E **67**, 046116 (2003).
- [11] R. O. Sokolovskii, Phys. Rev. B **61**, 36 (2000).
- [12] S. Romano and R. O. Sokolovskii, Phys. Rev. B **61**, 11379 (2000).
- [13] M. Blume, V. J. Emery, and R. B. Griffiths, Phys. Rev. A **4**, 1071 (1971).
- [14] A. Maciolek, M. Krech and S. Dietrich, Phys. Rev. E **69**, 036117 (2004).
- [15] D. J. Tulimieri, J. Yoon, and M. H. W. Chan, Phys. Rev. Lett. **82**, 121 (1999).
- [16] E. Lomba *et al.*, Phys. Rev. E **49**, 5169 (1994).
- [17] F. Lado and E. Lomba, Phys. Rev. Lett. **80**, 3535 (1998).
- [18] T. G. Sokolovska, Physica A **253**, 459 (1998).
- [19] F. Lado, E. Lomba, and J. J. Weis, Phys. Rev. E **58**, 3478 (1998).
- [20] T. G. Sokolovska and R. O. Sokolovskii, Phys. Rev. E **59**, R3819 (1999).
- [21] M. J. P. Nijmeijer and J. J. Weis, Phys. Rev. E **53**, 591 (1996).
- [22] J. J. Weis *et al.*, Phys. Rev. E **55**, 436 (1997).
- [23] M. J. P. Nijmeijer, A. Parola, and L. Reatto, Phys. Rev. E **57**, 465 (1998).
- [24] I. M. Mryglod, I. P. Omelyan, and R. Folk, Phys. Rev. Lett. **86**, 3156 (2001).
- [25] K. Moon and S. M. Girvin, Phys. Rev. Lett. **75**, 1328 (1995).
- [26] J. P. Hansen and I. R. McDonald, *Theory of Simple Liquids*, 2nd edn. (Academic, London, 1986).
- [27] N. Choudhury and S. K. Ghosh, J. Chem. Phys. **116**, 8517 (2002).
- [28] A. Z. Panagiotopoulos, Molec. Sim. **9**, 1 (1992).
- [29] A. M. Ferrenberg and R. H. Swendsen, Phys. Rev. Lett. **61**, 2635 (1988); **63**, 1195 (1989).
- [30] K. Binder, Rep. Prog. Phys. **60**, 487 (1997).
- [31] J. Zinn-Justin, *Quantum Field Theory and Critical Phenomena* (Clarendon, Oxford, 1983).